

Numerical Optimization of Pin-Fin Heat Sink with Forced Cooling

Y. T. Yang, H. S. Peng, and H. T. Hsu

Abstract—This study presents the numerical simulation of optimum pin-fin heat sink with air impinging cooling by using Taguchi method. L_9 (3^4) orthogonal array is selected as a plan for the four design-parameters with three levels. The governing equations are discretized by using the control-volume-based-finite-difference method with a power-law scheme on the non-uniform staggered grid. We solved the coupling of the velocity and the pressure terms of momentum equations using SIMPLEC algorithm. We employ the $k-\varepsilon$ two-equations turbulence model to describe the turbulent behavior. The parameters studied include fin height H (35mm-45mm), inter-fin spacing a , b , and C (2 mm-6.4 mm), and Reynolds number ($Re = 10000-25000$). The objective of this study is to examine the effects of the fin spacings and fin height on the thermal resistance and to find the optimum group by using the Taguchi method. We found that the fin spacings from the center to the edge of the heat sink gradually extended, and the longer the fin's height the better the results. The optimum group is $H_3a_1b_2c_3$. In addition, the effects of parameters are ranked by importance as a , H , c , and b .

Keywords—Heat sink, Optimum, Electronics cooling, CFD.

I. INTRODUCTION

THE rapid development of electronic technology causes the sizes of electronic components to shrink. The heat flux per unit area has increased dramatically over the past decade. Thus, the effective removal of heat has played an important role in ensuring a reliable operation of electronic components. Conventional electronics cooling normally used forced air cooling with heat sink showing superiority in terms of unit price, weight and reliability. A number of research scholars have examined the thermal and hydraulic characteristics of various heat sinks extensively. The steady-state forced-convective cooling of a horizontally based pin-fin assembly has been investigated experimentally by Haq et al. [1]. The overall pressure drop and the effect of the shroud clearance were examined. Ledezma et al. [2] performed an experimental, numerical and theoretical study of the heat transfer on a pin-finned plate. They demonstrated the optimization principle experimentally by comparing several spacing designs in the same air stream in a wind tunnel.

Moreover, the correlation equations for optimal fin-to-fin

Y. T. Yang is with the National Cheng Kung University, Tainan, 70101 Taiwan, (phone: 886-6-2757575-62172; fax: 886-6-235-2973; e-mail: ytyang@mail.ncku.edu.tw)

H. S. Peng was PhD student, graduated from National Cheng Kung University; currently he works in the industry.

H. T. Hsu was MSc student, graduated from National Cheng Kung University; currently he works in the industry.

spacing and the maximum thermal conductance were developed. Ledezma and Bejan [3] performed the experimental and numerical study of heat sinks with sloped plate fins. This study discussed the thermal performance on the orientation of the fin array and the tilting of the crests of the plate fins. Li et al. [4] and Li and Chen [5] investigated the thermal performance of pin-fin and plate-fin heat sinks with confined impingement cooling by using infrared thermography. The results show that the thermal resistance of the heat sinks decreases with the increased Reynolds number of the impinging jet. However, the reduction of the thermal resistance decreases gradually as the Reynolds number increases. Moreover, it revealed that the influence of fin width is more obvious than the fin height. In addition, the optimal impinging distance increases with the increasing Reynolds number. Finally, they concluded that the thermal performance of the pin-fin heat sinks is superior to that of the plate-fin heat sinks. Furthermore, the thermal performance of pin-fin heat sinks with air impingement cooling was performed numerically and experimentally by Li and Chen [6]. The effects of the fin geometry and the Reynolds number on the heat transfer of the heat sinks were also discussed. Brignoni and Garimella [7] demonstrated the experimental optimization of confined impinging air jets used in conjunction with a pin-fin heat sink. Enhancement factors for the heat sink relative to a bare surface were evaluated, and were in the range of 2.8 ~ 9.7, with the largest value being obtained for the largest single nozzle. Both the average heat transfer coefficients and the thermal resistance were expressed for the heat sink as a function of a Reynolds number, an air flow rate, a pumping power, and a pressure drop, to assist in optimizing the jet impingement configuration for given design constraints. Maveety and Hendricks [8] investigated the performance study of pin-fin heat sinks with impingement cooling which considered the effects of geometry, nozzle-to-heat sink vertical placement, material, and Reynolds number. The results revealed that there is an optimal nozzle-to-sink height and Reynolds number for which the heat dissipation is maximized. The best performance occurred when the dimensionless impingement distance was between 8 and 12, and when the Reynolds number was between 40000 and 50000. The results also presented that due to the higher spreading resistance efficiency of the carbon composite material, it led to more uniform cooling of the heat sink. Moreover, the influence of the nozzle-to-heat sink vertical placement on the thermal performance was reduced as the Reynolds number increased. The comparisons between numerical and experimental results for the cooling performance from a pin-fin heat sink with an

impinging air flow have been studied by Maveety and Jung [9]. The optimization studies were also discussed to quantify the effects of changing the fin shapes on the cooling performance. The numerical results illustrated a complex pressure gradient inside the fin array and a greater pressure gradient improved mixing and heat transfer. It also revealed that a complicated fluid motion with large pressure gradients generated vorticity, circulation and flow reversals. The enhancement of heat transfer from a discrete heat source in a confined air jet impingement was experimentally studied by El-Sheikh and Garimella [10]. A variety of pin-fin heat sinks were mounted on the heat source and the resulting enhancement was discussed. Relative to an unpinned heat sink, the heat transfer from the pinned ones was improved by 2.4 to 9.2 times. Due to the introduction of the heat sinks, the enhancement factors relative to the bare heat source varied from 7.5 to 72. Results for the average heat transfer coefficient were correlated as a function of the Reynolds number, fluid properties and geometric parameters of the heat sinks. The thermal performance of a pin-fin heat sink was studied theoretically and experimentally by Kobus and Oshio [11]. They carried out a theoretical model that has the capability of predicting the influence of various physical, thermal and flow parameters on the effective thermal resistance of a pin-fin array heat sink. Besides, the predictive capability of the theoretical model was verified by comparing with experimental data and was shown to be exceptionally good over the range of parameters. Kobus and Oshio [12] investigate the influence of thermal radiation on the thermal performance of a pin fin array heat sink theoretically and experimentally. A theoretical thermal radiation model was developed for predicting the effective thermal resistance of a fin array heat sink. The thermal and hydraulic behavior due to jet impingement on pin fin heat sinks was experimentally investigated by Issa and Ortega [13]. This study showed that the pressure loss coefficient increased with increasing pin density and pin diameter, and decreased with increasing pin height and clearance ratio. Moreover, the overall base-to-ambient thermal resistance decreased with the increasing Reynolds number, pin density and pin diameter. Duan and Muzychka [14] performed the experimental investigation of the thermal performance with four heat sinks of various impingement inlet widths, fin spacings, fin heights and airflow velocities. They developed a heat transfer model to predict the thermal performance of impingement air cooled plate fin heat sinks for design purposes. An experimental study was conducted to investigate the heat transfer from a parallel flat plate heat sink under a turbulent air jet impingement by Sansoucy et al. [15]. The forced convection heat transfer rates from a flat plate and from a flat plated heat sink under an impinging confined jet have been obtained. In addition, the experimental results were compared with the numerical predictions obtained in an earlier study. They concluded that the numerical analysis in a previous study was adequate for appraising the mean heat transfer rate in jet impingement for situations of thermal management of electronics.

Excluding numerical simulation or experimental studies, the entropy generation method was also utilized to evaluate or

optimize the thermal performance of the heat sink [16-20]. The procedure is based on the minimization of entropy generation resulting from heat transfer and pressure drop. The model demonstrates a rapid and stable procedure for obtaining optimum design/operational conditions without resorting to parametric analyses by using repeated iterations with a thermal analysis tool.

Moreover, several scholars have attempted to modify the fin shape to improve the thermal and hydraulic performance. The study of pin fin heat sink with different fin shape designs was performed by Yang and Peng [21], [22]. They designed the fins with un-uniform fin height and width to improve the thermal performance. The results demonstrated that the adequate fin shape design could enlarge the heat transfer area and decrease the flow resistance in the central region. It decreases the junction temperature and increases the enhancement of the thermal performance simultaneously. Sathé and Sammakia [23] and Shah et al. [24] conducted a study of a new and unique high-performance air-cooled impingement heat sink. The influences of the fin shape, particularly near the center of the heat sink were examined. The study revealed that the pressure drop can be reduced by cutting the fins in the central impingement zone without sacrificing heat transfer rates. It enhances not only the thermal performance but also the hydraulic performance of the sink. Shah et al. [25] extended the previous work by discussing the effect of the removal of a fin material from the end fins and the total number of fins, and the reduction in the size of the hub fan. They developed a new optimal heat sink design by using actual fan operating characteristics. Lorenzini and Moretti [26] analyzed the Y-shape fins and examined the geometries by varying the angle between the two arms of the Y and proposed new shape for the fins. Naphon and Sookkasem [27] investigated the heat transfer characteristics of tapered cylinder pin fin heat sinks experimentally and numerically. Ji et al. [28] studied the cooling performance of triangular folded fin heat sink. They discussed the influence of the fin pitch, the Reynolds number, and the fin height. The results showed that the cooling performance of triangular folded fin heat sinks depended significantly on the fin height, the fin pitch, and the Reynolds number. Moreover, the empirical correlations were developed to predict the heat transfer coefficient and pressure drop. The numerical predictions of heat transfer and flow characteristics of heat sinks with ribbed and dimpled surface have been done by Wee et al. [29]. The results showed that the heat transfer augmentation produced by the ribs is about 104% higher than that produced by the smooth-surface heat sink. But the ribs also produce higher static pressure variations, higher velocity gradients, and higher streamwise vorticity magnitudes. Applying dimples to heat sink surface gives a spatially averaged Nusselt number increase of 63%, with a pressure drop penalty which is much lower than the one produced by ribbed surfaces.

In the present study, the numerical simulations of pin-fin heat sinks with impingement cooling in thermal-fluid characteristics are investigated. The purpose of this study is to

examine the effects of the fin height and inter-fin spacing on the thermal performance of the heat sink.

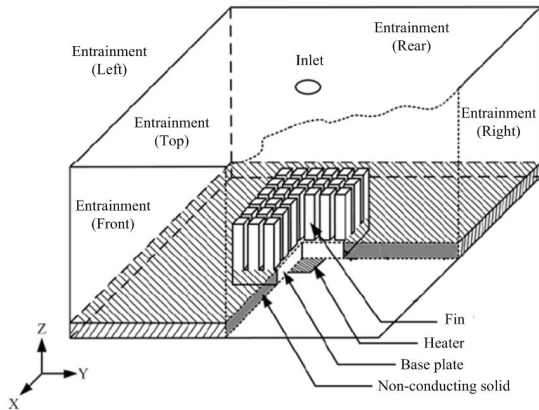


Fig. 1 Physical domain

II. MATHEMATICAL MODEL AND NUMERICAL METHOD

The schematic diagram of the geometry and the computational domain is shown in Fig. 1. The dimensions of the computational domain were based on the work by Li and Chen [6]. Taking advantage of the symmetry, the numerical simulations have been performed by considering only a one-quarter model of the physical domain. The boundary conditions for this problem are stated as follows. At the flow inlet, the air was uniformly induced downward with a constant temperature. The entrainment boundary conditions are used at the outlet. No slip conditions with thermally insulated are provided on all the other walls. At the bottom of the heat sink, a uniform constant heat flux is applied to the heating area. The adiabatic thermal boundary conditions are utilized at the outer perimeter of the bottom of heat sink except for the heating area.

The turbulent three dimensional Navier-Stokes and energy equations are solved numerically (using a finite difference scheme) combined with the continuity equation to simulate the thermal and turbulent flow fields. An eddy viscosity model is used to account for the effects of turbulence. The flow is assumed to be steady, incompressible, and three dimensional. The buoyancy and radiation heat transfer effects are neglected. In addition, the thermophysical properties of the fluid are assumed to be constant. The three dimensional governing equations of mass, momentum, turbulent kinetic energy, turbulent energy dissipation rate, and energy in the steady turbulent main flow using the standard $k-\varepsilon$ model are as follows:

Continuity equation

$$\frac{\partial \rho \bar{u}_i}{\partial x_i} = 0 \quad (1)$$

Momentum equation

$$\rho \bar{u}_j \frac{\partial \bar{u}_i}{\partial x_j} = -\frac{\partial \bar{p}}{\partial x_i} + \frac{\partial}{\partial x_j} \left[(\mu + \mu_t) \left(\frac{\partial \bar{u}_i}{\partial x_j} + \frac{\partial \bar{u}_j}{\partial x_i} \right) \right] \quad (2)$$

Energy equation of fluid

$$\rho \bar{u}_j \frac{\partial \bar{T}}{\partial x_j} = \frac{\partial}{\partial x_j} \left[\left(\frac{\mu_t}{\sigma_t} + \frac{\mu_s}{\sigma_s} \right) \frac{\partial \bar{T}}{\partial x_j} \right] \quad (3)$$

Energy equation of solid

$$\frac{\partial}{\partial x_i} \left(k_s \frac{\partial T}{\partial x_i} \right) = 0 \quad (4)$$

Transport equation for k

$$\rho \bar{u}_j \frac{\partial k}{\partial x_j} = \frac{\partial}{\partial x_j} \left[\left(\mu + \frac{\mu_t}{\sigma_k} \right) \frac{\partial k}{\partial x_j} \right] + \mu_t \left(\frac{\partial \bar{u}_i}{\partial x_j} + \frac{\partial \bar{u}_j}{\partial x_i} \right) \frac{\partial \bar{u}_i}{\partial x_j} - \rho \varepsilon \quad (5)$$

Transport equation for ε

$$\rho \bar{u}_j \frac{\partial \varepsilon}{\partial x_j} = \frac{\partial}{\partial x_j} \left[\left(\mu + \frac{\mu_t}{\sigma_\varepsilon} \right) \frac{\partial \varepsilon}{\partial x_j} \right] + C_1 \mu_t \frac{\varepsilon}{k} \left(\frac{\partial \bar{u}_i}{\partial x_j} + \frac{\partial \bar{u}_j}{\partial x_i} \right) \frac{\partial \bar{u}_i}{\partial x_j} - C_2 \rho \frac{\varepsilon^2}{k} \quad (6)$$

The Reynolds number of the impinging jet is defined as

$$Re = \frac{|W_m| d}{\nu} \quad (7)$$

where d denotes the diameter of nozzle.

As far as evaluating the efficiency of heat dissipation, thermal resistance is often used to rate the performances of the heat sink. The thermal resistance of the heat sink, R_{th} , can be defined by

$$R_{th} = \frac{T_{ave} - T_{in}}{Q} \quad (8)$$

where T_{ave} and T_{in} are the average temperature of the base of the heat sink and the temperature of the inlet fluid, respectively. Q is the heating power applied on the base of heat sink.

The coefficient of enhancement (COE) is defined to quantify the improvement in heat transfer rates due to the different types of the heat sink fins. This is expressed as

$$COE = \frac{Nu_{new}}{Nu_{origin}} \quad (9)$$

where the average Nusselt number Nu is calculated by

$$Nu = \frac{hd}{k_a} \quad (10)$$

and the average convection heat transfer coefficient h is calculated by

$$h = \frac{q''}{T_{base} - T_{in}} \quad (11)$$

Numerical approach

We employ a non-uniform and staggered grid system. A staggered grid arrangement is used in which the velocities are stored at a location on the control-volume faces. All other variables including pressure are calculated at the grid points. The numerical method used in the present study is based on the SIMPLEC algorithm [30]. Pressure and velocity correction schemes are implemented in the model algorithm to arrive at a converged solution when both the pressure and velocity satisfy the momentum and continuity equations. For non-linear problems, we employ the under-relaxation to avoid divergence in the iterative solutions. The resulting sets of discretized equations for each variable are solved by the line-by-line procedure which is the combination of the Tri-Diagonal Matrix Algorithm (TDMA) and the Gauss-Seidal iteration technique. The solution is considered to be converged when the normalized residual of the algebraic equation is less than a prescribed value of 10^{-3} .

Taguchi method

In the present study, all parameters influencing the thermal resistance and the pressure drop have not been investigated in details as it requires a large number of simulations and time taken. The Taguchi method developed by Genichi Taguchi is a useful method for systematically optimized designs. The number of simulations required for a whole analysis in the case of four three-level parameters can be reduced from 81 (3^4) to 9. The $L_9(3^4)$ orthogonal array can be adopted for further analyses of the sensitivity of each parameter. Table I and Table II list the values of four factors three levels and nine cases for $L_9(3^4)$ orthogonal array. The parameters affecting thermal resistance, namely fin height H , inter-fin spacing a , inter-fin spacing b , inter-fin spacing c (denote in Fig. 2) are inserted in columns A, B, C, and D. The purpose is to obtain the minimum thermal resistance. The performance statistics were chosen as the optimization criterion. It was used for “the smaller the better” situations, evaluated using the following equation:

$$S/N = -10 \log \left(\frac{\sum_{i=1}^n y_i^2}{n} \right) = -\log(\bar{y}^2 + S^2) \quad (12)$$

TABLE I
 $L_9(3^4)$ ORTHOGONAL ARRAY OF THE TAGUCHI METHOD

Case no.	Parameters and their levels			
	A	B	C	D
1	1	1	1	1
2	1	2	2	2
3	1	3	3	3
4	2	1	2	3
5	2	2	3	1
6	2	3	1	2
7	3	1	3	2
8	3	2	1	3
9	3	3	2	1

TABLE II
 FACTORS USED IN THE TAGUCHI METHOD

Parameters	Levels		
	1	2	3
A: Fin height (H) (mm)	35	40	45
B: Inter-fin spacing (a) (mm)	2	4.2	6.4
C: Inter-fin spacing (b) (mm)	2	4.2	6.4
D: Inter-fin spacing (c) (mm)	2	4.2	6.4

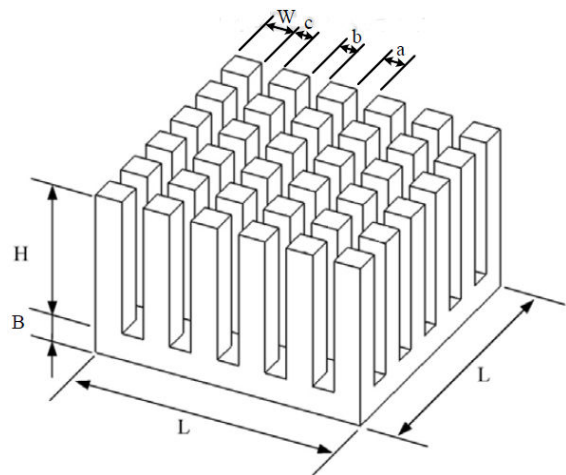


Fig. 2 Denotations of the pin fin heat sink

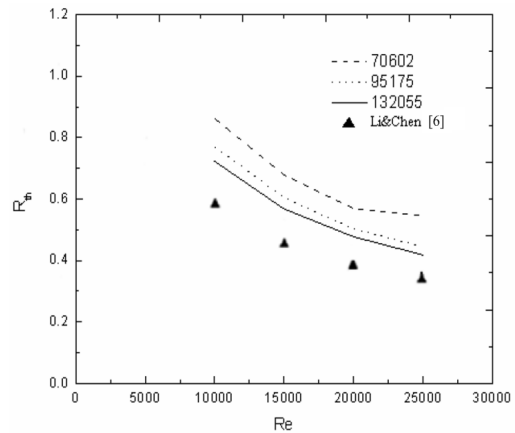


Fig. 3 Grid refinement

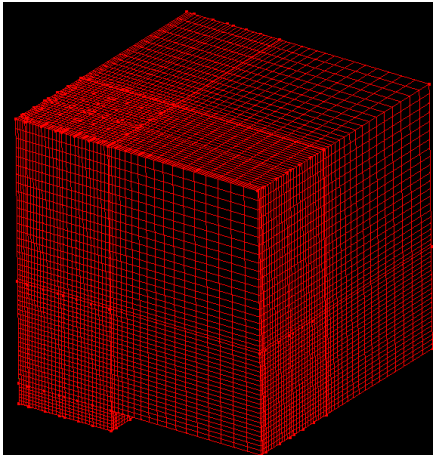


Fig. 4 The mesh distribution of computational domain (original design, mesh-95175)

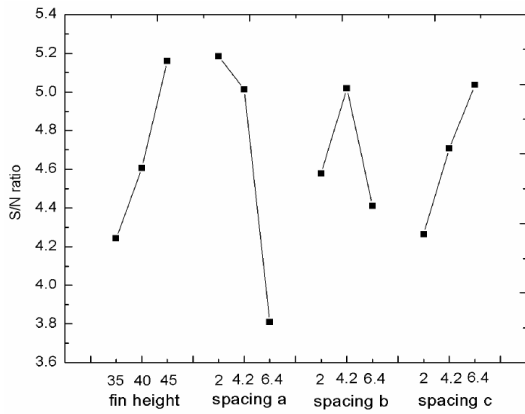


Fig. 5 The effect of each parameter on the thermal resistance (Re = 15000)

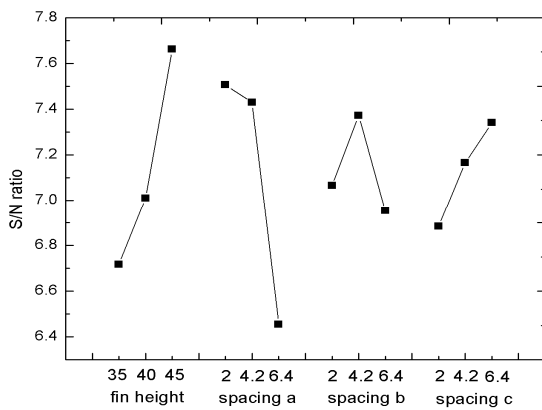


Fig. 6 The effect of each parameter on the thermal resistance (Re = 25000)

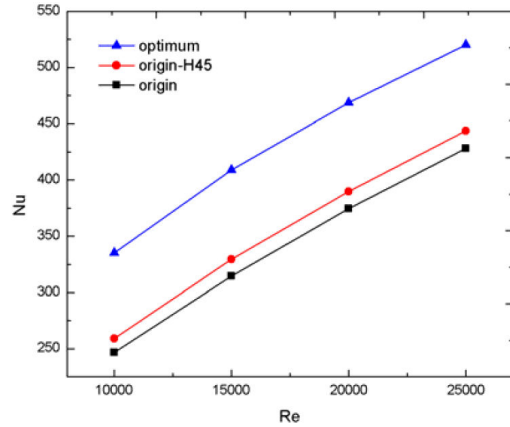


Fig. 7 Simulations of Nusselt number of three heat sinks as a function of Reynolds number

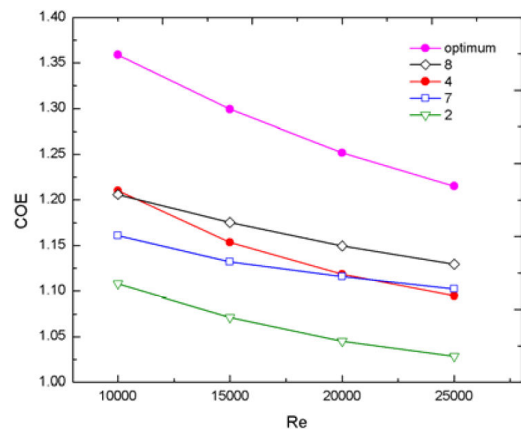
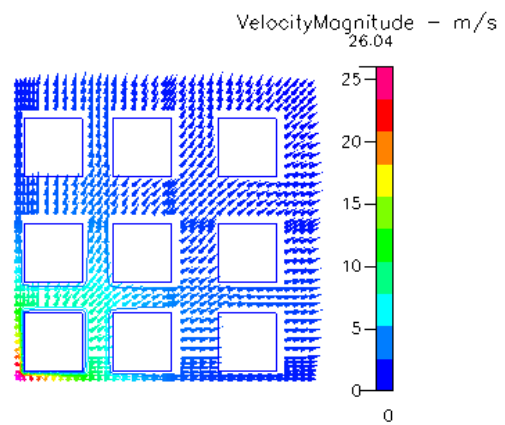
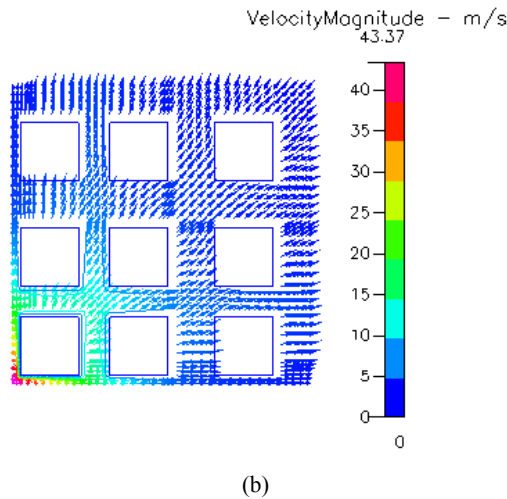


Fig. 8 Effects of the Reynolds number and the fin design (better than the original design) on COE

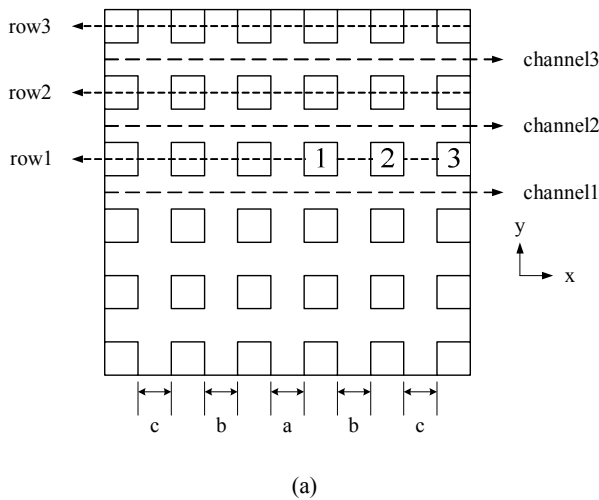


(a)

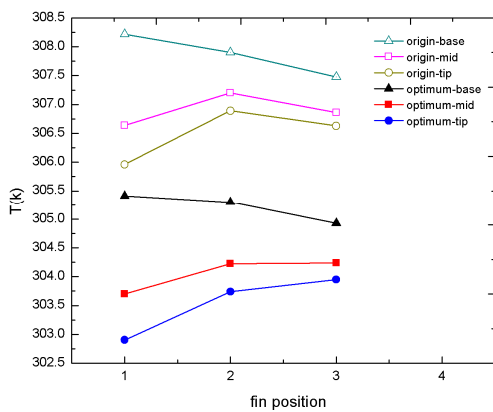


(b)

Fig. 9 Velocity field (optimum design, $z = 0.045\text{m}$) (a) $Re = 15000$,
 (b) $Re = 25000$



(a)



(b)

Fig. 10 (a) Different locations in the physical domain, (b) fin temperature distribution ($Re = 15000$, at row-1)

III. RESULTS AND DISCUSSION

The dimensions of the heat sink in this study were based on the work by Li and Chen [6]. Both the length and width of the

base of the heat sink are 80mm. The area of the heater is 40mm \times 40mm, which is in the center of the heat sink. The heating area is heated with heating power 20 W.

The parameters used in the grid refinement test were based on the uniform inter-fin spacing design and $H = 40\text{mm}$. A total number of meshes, 70602, 95175 and 132055 were employed to assess the grid independence. As shown in Fig. 3, the results of the grid sensitivity study showed that the simulations based on the 95175 meshes provide satisfactory numerical accuracy. A non-uniform and staggered grid system with a large concentration of nodes in regions of steep gradients, such as those close to the walls is employed. As seen in Fig. 4, the non-uniform grid system is chosen as a compromise between computational effort and accuracy.

From Table III and Fig. 5, it can be seen that the most effective parameters on the thermal resistance are found as follows: the inter-fin spacing (a), the fin height (H), the inter-fin spacing (c), and the inter-fin spacing (b). The thermal resistance decreases with increasing the fin height. Increasing the fin height enlarges the heat transfer area of the heat sink, which enhances the heat transfer rate. Hence, the thermal performance improved. The thermal resistance increases by increasing the inter-fin spacing a . The thermal resistance decreases when the inter-fin spacing b changes from 2mm to 4.2mm, and then increases when inter-fin spacing b changes from 4.2mm to 6.4mm. The effect of inter-fin spacing c is contrary to inter-fin spacing a . The thermal resistance decreases when increasing the inter-fin spacing c . It is important to enlarge the heat transfer area for efficient heat dissipation in the central region of the heat sink. Therefore, the inter-fin spacing a should be decreased in the center of the heat sink in order to increase the heat transfer area in the central region. The momentum of working fluid is weak around the rim of the heat sink. Hence, the inter-fin spacing c should be increased to reduce the flow resistance and allow more working fluid to flow out. Fig. 6 depicts the effect of each parameter on the thermal resistance at $Re = 25000$. As shown in the figure, the trends of the S/N ratio are similar to the previous case.

Fig. 7 shows the simulations of the Nusselt number of three heat sinks as a function of the Reynolds number. From Fig. 7, it is seen that increasing the Reynolds number increases the Nusselt number. However, the increment of the Nusselt number decreases gradually as the Reynolds number increases. The figure also shows the comparison of the Nusselt number between the original and optimal designs. The result of optimum condition of the Nusselt number is much higher than the original designs.

The effects of the Reynolds number and the fin design (better than the original design) on COE is shown in Fig. 8. Although the fin height of case 9 is higher than cases 2 and 4, the COE of case 9 is lower. This is because the flow penetration into the heat sink becomes weaker due to the increased flow resistance. Hence, the inter-fin spacing should be designed for more working fluid to flow into the heat sink. Moreover, it can be seen that COE decreases when the Reynolds number increases. The enhancement of the heat

transfer by increasing the Reynolds number may have a limitation.

Table IV shows the temperature comparison between the original and optimum designs at different heating power. When the heating power is 20 W, the temperature difference between original and optimum design is about 4K at $Re = 10000$ and 1.4K at $Re = 25000$. When the heating power increased from 20 W to 40 W, the temperature difference between original and optimum design is more obvious.

As shown in Fig. 9, the working fluid flows directly into the heat sink and accelerates as it enters the inter-fin spacing as a result of the area contraction. Then, the fluid is decelerated giving rise to increased static pressure and flow resistance. The fluid flow changes direction to flow along the base plate of the heat sink. The velocity field decreases from top to bottom and from inner to outer. Fig. 10 shows the temperature distribution at row-1. The main influence of impinging jet on the heat sink is at the central region. Hence, as shown in the figure, the temperature of the tip of fin-1 is lower than other fins. Besides, the heat dissipations are centrally concentrated on the fin base. The flow penetration into the center of the heat sink becomes weaker due to the flow resistance. Therefore, the temperature of the bottom of fin-1 is much higher than fin-2 and fin-3. In addition, the velocity of fluids in channel-2 and channel-3 are about the same. The temperature difference between fin-2 and fin-3 appeared to be minimal.

TABLE III
THE S/N VALUES AND EFFECTS OF EACH PARAMETER

	A	B	C	D
Level-1	4.243146	5.185925	4.577446	4.264682
Level-2	4.606064	5.014490	5.020508	4.706879
Level-3	5.159856	3.808650	4.411112	5.037505
Effect	0.916709	1.377276	0.609395	0.772823
Rank	2	1	4	3
Best	5.159856	5.185925	5.020508	5.037505

TABLE IV
THE AVERAGED TEMPERATURE OF BASE PLATE

Heating power	Fin shape	T_{ave} (K)			
		Re=10000	Re=15000	Re=20000	Re=25000
$Q = 20$ W	Origin	311.166	307.808	305.874	304.592
	Optimum	307.173	305.117	303.922	303.115
$Q = 60$ W	Origin	343.874	333.871	326.432	324.03
	Optimum	331.444	325.171	321.425	318.787

IV. CONCLUSION

The present study provides valuable information on the pin-fin heat sink with air impinging cooling by numerical simulations with the Taguchi method. The parameters affecting thermal performance have been systematically investigated by using L_9 (3^4) orthogonal array. The governing equations are discretized by using the control-volume-based-finite-difference method with a power-law scheme on an orthogonal non-uniform staggered grid. The coupling of the velocity and the pressure terms of momentum equations are solved by the SIMPLEC algorithm. The $k-\epsilon$ two-equations turbulence model is employed to

describe the turbulent structure and behavior. The parameters studied include fin height H (35mm, 40mm, 45mm), inter-fin spacing a (2mm, 4.2mm, 6.4mm), inter-fin spacing b (2mm, 4.2mm, 6.4mm), and inter-fin spacing c (2mm, 4.2mm, 6.4mm). The results of the present study are described as follows.

- 1) The optimum group is $H_3a_1b_2c_3$, i.e. $H = 45$ mm, $a = 2$ mm, $b = 4.2$ mm, $c = 6.4$ mm.
- 2) The effects of parameters are ranked by importance as a , H , c , and b .
- 3) It is found that an adequate arrangement of inter-fin spacing could increase the Nusselt number and COE. The increments of the Nusselt number and COE decrease gradually as the Reynolds number increases. At high Reynolds numbers, the effects of geometries are decayed.

ACKNOWLEDGMENT

We would like to thank the National Science Council of the Republic of China for supporting this project under contract No. NSC 96-2221-E-006-161-MY2.

REFERENCES

- [1] R. F. B. Haq, K. Akintunde, and S. D. Probert, "Thermal Performance of a Pin-Fin Assembly," *Int. J. Heat Fluid Flow*, vol. 16, pp. 50-55, 1995.
- [2] G. Ledezma, A. M. Morega, and A. Bejan, "Optimal Spacing between Pin Fins with Impinging Flow," *J. Heat Transfer*, vol. 118, pp. 570-577, 1996.
- [3] G. Ledezma, and A. Bejan, "Heat Sinks with Sloped Plate Fins in Natural and Forced Convection," *Int. J. Heat Mass Transfer*, vol. 39, no. 9, pp. 1773-1783, 1996.
- [4] H. Y. Li, S. M. Chao, and G. L. Tsai, "Thermal Performance Measurement of Heat Sinks with Confined Impinging Jet by Infrared Thermography," *Int. J. Heat Mass Transfer*, vol. 48, pp. 5386-5394, 2005.
- [5] H. Y. Li, and K. Y. Chen, "Thermal Performance of Plate-Fin Heat Sinks under Confined Impinging Jet Conditions," *Int. J. Heat Mass Transfer*, vol. 50, pp. 1963-1970, 2007.
- [6] H. Y. Li, and K. Y. Chen, "Thermal-Fluid Characteristics of Pin-Fin Heat Sinks Cooled by Impinging Jet," *J. Enhanced Heat Transfer*, vol. 12, no. 2, pp. 189-201, 2005.
- [7] L. A. Brignoni, and S. V. Garimella, "Experimental Optimization of Confined Air Jet Impingement on a Pin Fin Heat Sink," *IEEE Trans. Compon. Packaging Technol.*, vol. 22, no. 3, pp. 399-404, 1999.
- [8] J. G. Maveety, and J. F. Hendricks, "A Heat Sink Performance Study Considering Material, Geometry, Reynolds Number with Air Impingement," *J. Electron. Packag.*, vol. 121, pp. 156-161, 1999.
- [9] J. G. Maveety, and H. H. Jung, "Design of an Optimal Pin-Fin Heat Sink with Air Impingement Cooling," *Int. Commun. Heat Mass Transfer*, vol. 27, no. 2, pp. 229-240, 2000.
- [10] H. A. El-Sheikh, and S. V. Garimella, "Enhancement of Air Jet Impinging Heat Transfer Using Pin-Fin Heat Sinks," *IEEE Trans. Compon. Packaging Technol.*, vol. 23, no. 2, pp. 300-308, 2000.
- [11] C. J. Kobus, and T. Oshio, "Development of a Theoretical Model for Predicting the Thermal Performance Characteristics of a Vertical Pin-fin Array Heat Sink under Combined Forced and Natural Convection," *Int. J. Heat Mass Transfer*, vol. 48, pp. 1053-1063, 2005.
- [12] C. J. Kobus, and T. Oshio, "Predicting the Thermal Performance Characteristics of Staggered Vertical Pin Fin Array Heat Sinks under Combined Mode Radiation and Mixed Convection with Impinging Flow," *Int. J. Heat Mass Transfer*, vol. 48, pp. 2684-2696, 2005.
- [13] J. S. Issa, and A. Ortega, "Experimental Measurements of the Flow and Heat Transfer of a Square Jet Impinging on an Array of Square Pin Fins," *J. Electron. Packag.*, vol. 128, pp. 61-70, 2006.
- [14] Z. Duan, and Y. S. Muzychka, "Experimental Investigation of Heat Transfer in Impingement Air Cooled Plate Fin Heat Sinks," *J. Electron. Packag.*, vol. 128, pp. 412-418, 2006.
- [15] E. Sansoucy, P. H. Oosthuizen, and G. R. Ahmed, "An Experimental

- Study of the Enhancement of Air-Cooling Limits for Telecom/Datacom Heat Sink Applications Using an Impinging Air Jet," *J. Electron. Packag.*, vol. 128, pp. 166-171, 2006.
- [16] J. R. Culham, and Y. S. Muzychka, "Optimization of Plate Fin Heat Sinks Using Entropy Generation Minimization," *IEEE Trans. Compon. Packaging Technol.*, vol. 24, no. 2, pp. 159-165, 2001.
- [17] W. W. Lin, and D. J. Lee, "Second-law Analysis on a Flat Plate-Fin Array under Crossflow," *Int. Commun. Heat Mass Transfer*, vol. 27, no. 2, pp. 179-190, 2000.
- [18] S. Z. Shuja, S. M. Zubair, and M. S. Khan, "Thermoeconomic Design and Analysis of Constant Cross-sectional Area Fins," *Heat Mass Transfer*, vol. 34, pp. 357-364, 1999.
- [19] W. A. Khan, J. R. Culham, and M. M. Yovanovich, "Optimization of Pin-fin Heat Sinks Using Entropy Generation Minimization," *ITHERM*, August, vol. 1, pp. 259-267, 2004.
- [20] K. Ogiso, "Assessment of Overall Cooling Performance in Thermal Design of Electronics Based on Thermodynamics," *J. Heat Transfer*, vol. 123, pp. 999-1005, 2001.
- [21] Y. T. Yang, and H. S. Peng, "Numerical Study of Pin-Fin Heat Sink with Un-uniform Fin Height Design," *Int. J. Heat Mass Transfer*, vol. 51, no. 19-20, pp. 4788-4796, 2008.
- [22] Y. T. Yang, and H. S. Peng, "Numerical Study of the Heat Sink with Un-uniform Fin Width Designs," *Int. J. Heat Mass Transfer*, vol. 52, no. 15-16, pp. 3473-3480, 2009.
- [23] S. B. Sathe, and B. G. Sammakia, "An Analytical Study of the Optimized Performance of an Impingement Heat Sink," *J. Electron. Packag.*, vol. 126, pp. 528-534, 2004.
- [24] A. Shah, B. G. Sammakia, H. Srihari, and K. Ramakrishna, "A Numerical Study of the Thermal Performance of an Impingement Heat Sink-Fin Shape Optimization," *IEEE Trans. Compon. Packaging Technol.*, vol. 27, no. 4, pp. 710-717, 2004.
- [25] A. Shah, B. G. Sammakia, K. Srihari, and K. Ramakrishna, "Optimization Study for a Parallel Plate Impingement Heat Sink," *J. Electron. Packag.*, vol. 128, pp. 311-318, 2006.
- [26] G. Lorenzini, and S. Moretti, "Numerical Analysis on Heat Removal from Y-shaped Fins: Efficiency and Volume Occupied for a New Approach to Performance Optimisation," *Int. J. Therm. Sci.*, vol. 46, pp. 573-579, 2007.
- [27] P. Naphon, and A. Sookkasem, "Investigation on Heat Transfer Characteristics of Tapered Cylinder Pin Fin Heat Sinks," *Energy Conv. Manag.*, vol. 48, pp. 2671-2679, 2007.
- [28] T. H. Ji, S. Y. Kim, and J. M. Hyun, "Pressure Drop and Heat Transfer Correlations for Triangular Folded Fin Heat Sinks," *IEEE Trans. Compon. Packaging Technol.*, vol. 30, no. 1, pp. 3-8, 2007.
- [29] H. Wee, Q. Zhang, P. M. Ligrani, and S. Narasimhan, "Numerical Predictions of Heat Transfer and Flow Characteristics of Heat Sinks with Ribbed and Dimpled Surfaces in Laminar Flow," *Numer. Heat Transf. A-Appl.*, vol. 53, pp. 1156-1175, 2008.
- [30] J. P. van Doormaal, and F. D. Raithby, "Enhancements of the SIMPLE method for predicting incompressible fluid flows," *Numer. Heat Transf.*, vol. 7, pp. 147-163, 1984.



Yue-Tzu Yang is a Professor at the Department of Mechanical Engineering, National Cheng Kung University, Taiwan, ROC. She received her Ph.D. in mechanical engineering from the University of Liverpool, UK in 1990. Her research interests include numerical simulations of turbulent flow, heat transfer enhancement, and electronic cooling.